MOLECULAR CARCINOGENESIS 49:464–475 (2010)

5,7,3′-Trihydroxy-3,4′-Dimethoxyflavone-Induced Cell Death in Human Leukemia Cells Is Dependent on Caspases and Activates the MAPK Pathway

Fernando Torres,[1,2] José Quintana,[1,2] and Francisco Estévez[1,2]*

[1]*Department of Biochemistry and Molecular Biology, University of Las Palmas de Gran Canaria, Las Palmas de Gran Canaria, Spain*
[2]*Instituto Canario de Investigación del Cáncer, Las Palmas de Gran Canaria, Spain*

Flavonoids are polyphenolic compounds which display a vast array of biological activities and are promising anticancer agents. In this study we investigated the effect of 5,7,3′-trihydroxy-3,4′-dimethoxyflavone (THDF) on viability of nine human tumor cell lines and found that it was highly cytotoxic against leukemia cells. THDF induced G_2–M phase cell-cycle arrest and apoptosis through a caspase-dependent mechanism involving cytochrome *c* release, processing of multiple caspases (caspase-3, -6, -7, and -9) and cleavage of poly(ADP-ribose) polymerase. Overexpression of the protective mitochondrial proteins Bcl-2 and Bcl-x_L conferred partial resistance to THDF-induced apoptosis. This flavonoid induced the phosphorylation of members of the mitogen-activated protein kinases (MAPKs) family and cell death was attenuated by inhibition of c-*jun* N-terminal kinases/stress-activated protein kinases (JNK/SAPK) and of extracellular signal-regulated kinases (ERK) 1/2. In the present study we report that THDF-induced cell death is mediated by an intrinsic dependent apoptotic event involving mitochondria and MAPKs, and through a mechanism independent of the generation of reactive oxygen species. The results suggest that THDF could be useful in the development of novel anticancer agents.

Key words: apoptosis; flavonoids; cell-cycle arrest; mitogen-activated protein kinases; c-*jun* N-terminal kinases; extracellular signal-regulated kinases

INTRODUCTION

Flavonoids are phenylbenzo-γ-pyrones derivatives which display a vast array of biological activities and are among the most promising anticancer agents [1]. One of the best-studied bioflavonoids is quercetin (3,3′,4′,5,7-pentahydroxyflavone). This compound potentiates the cytotoxic action of 1-β-D-arabinofuranosylcytosine [2] and inhibits cell invasion and induces apoptosis [3]. Many anticancer compounds have been shown to cause the death of sensitive cells through the induction of apoptosis. Essential executioners of apoptosis are the caspases, a family of conserved cysteine aspartate-specific proteases [4], generally synthesized as inactive proenzymes or zymogens which are activated by proteolytic cleavage. In general, two major pathways for apoptosis have been described [5]. In the extrinsic (or death receptor) pathway, apoptosis is mediated by death receptors (such as tumor necrosis factor or Fas receptors) [6] and involves caspase-8 activation, while in the intrinsic (or mitochondrial) pathway diverse proapoptotic signals lead to the release of cytochrome *c* from mitochondria to cytoplasm that promotes the assembly of apoptosome and caspase-9 activation. Since caspase-3 is responsible for cleaving specific cellular proteins during apoptosis [7] both pathways converge to this level and therefore caspase-8 and -9 cleave and activate the proenzyme. A great number of studies indicate that apoptosis can also be mediated by the endoplasmic reticulum signaling pathway [8] and it may occur independently of caspase activation [9].

Mitogen-activated protein kinases (MAPKs) are a family of serine/threonine protein kinases that are activated by mitogens or stress conditions and play an essential role in a diverse array of cellular functions, including proliferation, differentiation, stress responses, and apoptosis [10]. Mammalian

Abbreviations: MAPKs, mitogen-activated protein kinases; ERK, extracellular signal-regulated kinases; JNK, c-*jun* N-terminal kinases; SAPK, stress-activated protein kinase; $p38^{MAPK}$, p38 mitogen-activated protein kinases; THDF, 5,7,3′-trihydroxy-3,4′-dimethoxyflavone; ROS, reactive oxygen species; PARP, poly(ADP-ribose) polymerase; PBMC, peripheral blood mononuclear cells; IC_{50}, 50% inhibition of cell growth; JC-1, 5,5′,6,6′-tetrachloro-1,1′,3,3′-tetraethylbenzimidazolylcarbocyanine iodide; $\Delta\Psi_m$, mitochondrial membrane potential; H_2-DCF-DA, 2′,7′-dichlorodihydrofluorescein diacetate; MEK, mitogen-activated extracellular kinases; MKPs, MAPK phosphatases.

*Correspondence to: Plaza Dr Pasteur s/n, Las Palmas de Gran Canaria 35016, Spain.

Received 11 September 2009; Revised 4 December 2009; Accepted 28 December 2009

DOI 10.1002/mc.20619

Published online 19 February 2010 in Wiley InterScience (www.interscience.wiley.com)

MAPKs comprise three major groups, which are classified on the basis of sequence similarity, differential activation by agonists, and substrate specificity. These are the extracellular signal-regulated kinases (ERK) 1/2, the c-*jun* N-terminal kinases/stress-activated protein kinases (JNK/SAPK), and the p38 MAPKs ($p38^{MAPK}$). Activation of MAPKs requires dual phosphorylation of threonine and tyrosine residues in the catalytic domain by specific MAPK kinases (MAPKKs). ERK1/2 is predominantly activated by growth factors or mitogens leading to cell differentiation, growth, and survival. In contrast, JNK/SAPK and $p38^{MAPK}$ are preferentially activated in response to stress conditions and are often associated with apoptosis [11], although under certain conditions both kinases may induce anti-apoptotic, proliferative, and cell survival signals [12].

In a previous report, we described the cytotoxicity of 22 flavonoids in five human tumor cell lines and reported that the methylation of hydroxyl group at position C3 of quercetin yields a compound with a higher antiproliferative activity [13]. In the present study we have found that a derivative of quercetin, 3′,5,7-trihydroxy-3,4′-dimethoxyflavone (THDF), displays higher cytotoxic properties than the natural flavonoid in human leukemia cell lines and induces cell death by caspase activation which is associated with cytochrome *c* release. We have also evaluated whether the MAPK cascade and the reactive oxygen species (ROS) generation are involved in the mechanism of action.

MATERIALS AND METHODS

Reagents

THDF was from Extrasynthese (Genay Cedex, France). Antibodies for poly(ADP-ribose) polymerase (PARP), caspase-3, -8, and -9 were purchased from Stressgen (Victoria, British Columbia, Canada). Antibodies for cytochrome *c*, Bax, and caspase-7 were purchased from BD Pharmingen (San Diego, CA). Anticaspase-6 monoclonal antibody was from Medical and Biological Laboratories (Nagoya, Japan). Anti-Bcl-2 monoclonal antibody was from Santa Cruz Biotechnology (Santa Cruz, CA). Anticytochrome *c* oxidase (Cox IV) antibody was purchased from Abcam (Cambridge, UK). Anti-JNK/SAPK, antiphospho-JNK/SAPK (phospho T183 + Y185), anti-p44/42 MAPK, antiphospho-p44/p42 MAPK (T202/Y204), anti-$p38^{MAPK}$, and antiphospho-$p38^{MAPK}$ (T180/Y182) antibodies were purchased from New England BioLabs (Cell Signaling Technologies, Beverly, MA). Secondary antibodies were from GE Healthcare (Little Chalfont, UK). All other chemicals were obtained from Sigma (St. Louis, MO).

Cell Culture

The human leukemia HL-60, U937, and Jurkat cells and human SK-MEL-1 melanoma cells were grown as previously described [13–15]. Human leukemia Molt-3 cells were cultured in RPMI 1640 containing 2 mM L-glutamine supplemented with 10% (v/v) heat-inactivated fetal bovine serum. The human adenocarcinoma A549 cell line was cultured in Dulbecco's modified Eagle's medium containing 10% (v/v) heat-inactivated fetal bovine serum, 2 mM L-glutamine, 100 U/mL penicillin, 100 μg/mL streptomycin. Human peripheral blood mononuclear cells (PBMC) were isolated from heparin-anticoagulated blood of healthy volunteers by centrifugation with Ficoll-Paque Plus (GE Healthcare BioSciences AB, Uppsala, Sweden). PBMC are normal cells in a physiological G_0 state. PBMC grow in size, synthesize DNA, and eventually proliferate in the presence of phytohemagglutinin (PHA, 2 μg/mL for 48 h) [16].

HL-60 cells transfected with the pSFFV-neo plasmid (HL-60/neo) and/or pSFFV-bcl-x_L plasmid (HL-60/Bcl-x_L) (donated by Dr. Angelika Vollmar, Department of Pharmacy, Center of Drug Research, University of Munich, Germany, and which were established by Dr. K.N. Bhalla, Medical College of Georgia Cancer Center, GA) and the U937 cell line overexpressing human Bcl-2 (kindly provided by Dr. Jacqueline Bréard, INSERM U749, Faculté de Pharmacie Paris-Sud, Châtenay-Malabry, France) were cultured as described [17].

Cytotoxicity of THDF on Human Tumor Cells and Human Normal Peripheral Blood Mononuclear Cells

The cytotoxicity of THDF on human tumor and human PBMC cells was analyzed as previously described [13]. Concentrations inducing a 50% inhibition of cell growth (IC_{50}) were determined graphically for each experiment by a nonlinear regression using the curve-fitting routine of the computer software Prism™ 2.0 (GraphPad) and the equation derived by De Lean and co-workers [18]. Values are means ± SE from at least three independent experiments, each performed in triplicate.

Evaluation of Apoptosis

Fluorescent microscopy, flow cytometric analysis of propidium iodide-stained nuclei, and DNA fragmentation assay were performed as described [17]. Apoptosis was also determined by translocation of phosphatidylserine to the cell surface using an Annexin V-FITC apoptosis detection kit (BD Pharmingen) according to the manufacturer's protocol.

Analysis of DNA Fragmentation

A late biochemical hallmark of apoptosis is the fragmentation of the genomic DNA. It is an irreversible event and occurs before changes in plasma membrane permeability. DNA isolation and gel electrophoresis were performed as described previously [13].

Transmission Electron Microscopy (TEM)

Cells were treated with THDF for 24 h, harvested, and fixed (2.5% glutaraldehyde in 0.2 M sodium phosphate buffer, pH 7.2) for 24 h at 4°C. Then, cells were washed three times with sodium phosphate buffer, postfixed in 1% OsO_4 for 4 h at 4°C, and washed with distilled water. Cells were embedded in Epon 812 after dehydratation in ethanol. Ultrathin sections were counterstained with uranyl acetate and lead citrate before observations with a Zeiss EM 912 transmission electron microscope. Pictures were taken with a Proscan Slow-scan CCD-Camera for TEM.

Western Blot Analysis

Immunoblot analysis of caspase-9, -8, -7, -6, -3, PARP, and MAPKs was performed as previously described [17]. Release of cytochrome *c* from mitochondria was detected as described [15].

Assay of Caspase Activity

Caspase activity was performed as described previously [13].

Analysis of Mitochondrial Membrane Potential $\Delta\Psi_m$

The membrane potential was measured by FACS using the fluorochrome 5,5′,6,6′-tetrachloro-1,1′,3,3′-tetraethylbenzimidazolylcarbocyanine iodide (JC-1) as previously described [17]. Cells were treated with THDF (10 μM) for different time periods and incubated with the fluorescent probe JC-1 (10 μM) for the last 30 min. JC-1 exists as a monomer at low values of $\Delta\Psi_m$ (green fluorescence; emission, 527 nm) while it forms aggregates at high $\Delta\Psi_m$ (orange fluorescence; emission, 590 nm). Flow cytometric analysis was carried out using a Coulter EPICS^{TM} cytometer (Beckman Coulter, Miami, FL).

Intracellular Reactive Oxygen Species (ROS) Determination

Intracellular ROS were detected by flow cytometry using 2′,7′-dichlorodihydrofluorescein diacetate (H_2-DCF-DA). This compound is deacetylated by intracellular esterase and converted to nonfluorescent 2′,7′-dichlorodihydrofluorescein (H_2-DCF), which is rapidly oxidized to the highly fluorescent compound 2′,7′-dichlorofluorescein (DCF) in the presence of ROS (especially hydrogen peroxide and lipid hydroperoxides). HL-60 cells were treated with or without THDF for 15–120 min, and then H_2-DCF-DA (8 μM) was added and incubated for 30 min. The cells were then washed and resuspended in 1 mL phosphate-buffered saline (PBS). Flow cytometric analysis was carried out within 1 h using a Coulter EPICS^{TM} cytometer. In each study, 10 000 cells were counted. Fluorescence of DCF was detected at an excitation and emission wavelengths of 488 and 530 nm, respectively.

Statistical Analysis

Statistical significance of differences between means of control and treated samples were calculated using Student's *t*-test. *P*-values of <0.05 were considered significant.

RESULTS

THDF Inhibits Cell Viability of Human Tumor Cell Lines and Lack of Cytotoxicity on Normal Human Lymphocytes

In the present study, we examined the effects of THDF (Figure 1A) on the growth of nine human tumor cell lines and found that it displays strong cytotoxic properties (Table 1). Human myeloid (HL-60 and U937) and lymphoid (Jurkat and Molt-3) leukemia cell lines and cell lines overexpressing Bcl-2 (U937/Bcl-2) and Bcl-x_L proteins (HL-60/Bcl-x_L) were, in general, the most sensitive to THDF-induced cytotoxicity while human adenocarcinoma A549 ($IC_{50} = 10.8 \pm 2.4$ μM) and human melanoma SK-MEL-1 cell lines ($IC_{50} = 13.9 \pm 2.5$ μM) were more resistant (Figure 1B). Control experiments with normal quiescent lymphocytes showed no appreciable toxicity up to 10 μM THDF for 24 h (Figure 1C). Since HL-60 and U937 cells were especially sensitive to the antiproliferative effect of THDF, further studies were performed on these cell lines.

THDF Induces G_2–M Arrest and Apoptosis on Human Myeloid Leukemia Cells

To determine whether THDF-induced cytotoxicity involves alterations in cell-cycle progression, flow cytometric analyses were included in this study. As shown (Table 2, Figure 2A) THDF caused a significant G_2–M arrest at the expense of G_1 phase cell population at 6–12 h of treatment on both cell lines and this effect invariably diminished with increased treatment time (24 h) in HL-60 cells. The percentage of cells in G_2–M phase increased from ~25% in control cells to 44% after treatment with THDF for 12 h. Moreover, the percentage of hypodiploid cells (i.e., sub-G_1 fraction) increased about fivefold in THDF-treated HL-60 compared with control cells after 24 h exposure at a concentration as low as 1 μM (Figure 2A). THDF showed a similar trend in G_2–M arrest in U937 cells and this effect was sustained until 24 h. Maximal levels of apoptotic cells (approximately fivefold increase with respect to control) were observed at 12 h with 3 μM THDF in U937 or at 24 h with 1 μM THDF in HL-60 (Table 2). Taken together, these results indicate that THDF induces cell-cycle arrest in the G_2–M phase and apoptosis on human myeloid leukemia HL-60 and U937 cells.

When cells were incubated with THDF, the DNA showed the typical fragmentation patterns formed by internucleosomal hydrolysis of chromatin thus confirming the apoptosis-inducing effects (Figure 2B). Fluorescence microscopy experiments on HL-60 and U937 cells clearly demonstrate an increase of

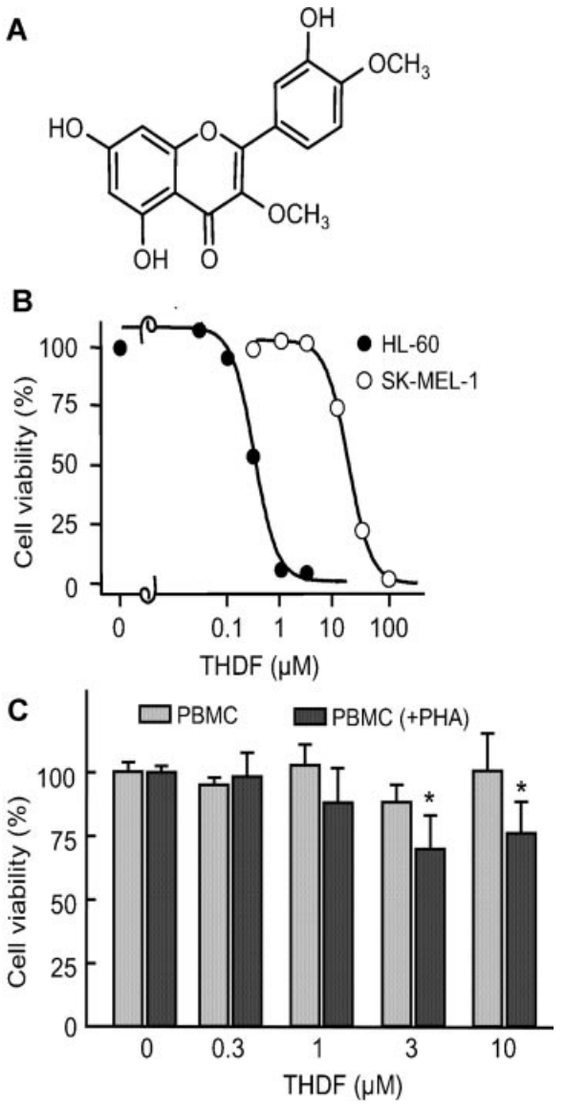

Figure 1. (A) Chemical structure of THDF. (B) Effect of THDF on human HL-60 and SK-MEL-1 cell viability. Cells were cultured in the presence of the indicated concentrations of THDF for 72 h, and thereafter cell viability was determined by the 3-(4,5-dimethyl-2-thyazolyl-)-2,5-diphenyl-2*H*-tetrazolium bromide assay (MTT). The results of a representative experiment are shown. Each point represents the mean of triplicate determinations. (C) Effect of THDF on proliferation of normal PBMCs. Quiescent and phytohemagglutinin-activated healthy human PBMC were cultured in presence of the indicated concentrations of THDF for 24 h. Values represent mean ± SE of three independent experiments each performed in triplicate. $*P < 0.05$, significantly different from untreated control.

condensed and fragmented chromatin, which is typical of apoptotic cells (Figure 2C). A significant number of apoptotic cells was already detected at 12 h of treatment and increased in a time-dependent manner (results not shown). THDF treatment also led to the exposure of phosphatidylserine on the outside of the plasma membrane as detected by Annexin V-FITC staining in both cell lines (Figure 2D). We also used transmission electronic microscopy to visualize the apoptosis-associated ultrastructural changes. Cells with fragmented and/or condensed nuclei characteristic of apoptotic cells were clearly visible as shown in Figure 2E. THDF-treated cells showed a dense perinuclear condensation and also abundant vacuoles.

Effects of THDF on Mitochondrial Cytochrome *c* Release and on Caspases and PARP Processing

To determine whether caspases were involved in the response of the cells to THDF, we examined whether this flavonoid induces proteolytic processing of caspases and PARP cleavage. To this end, HL-60 and U937 cells were treated with 3 μM THDF for various time durations or with increasing concentrations of this compound, and initiators (caspase-9 and -8) and executioners (caspase-7, -6, and -3) caspases were determined by Western blot using antibodies that bind both the proenzyme (caspase precursors) and the cleaved caspases. We used concentrations 3- to 10-fold higher than the antiproliferative IC_{50} values in order to identify the primary targets and early mechanism of action of THDF. The results indicate that THDF stimulates the cleavage of inactive procaspase-9 to the active 35–37 kDa fragment. This was clearly visible at 12 h of treatment in both cell lines. We also evaluated the potential contribution of the extrinsic apoptotic pathway. As shown in Figure 3A, THDF did not induce a significant procaspase-8 processing. Hydrolysis of this zymogen was only detected at longer incubation times (24 h) for treatments with the highest concentration (10 μM).

As caspase-3 is the main effector caspase we also analyzed whether THDF induces hydrolysis of the zymogen. Cleavage of procaspase-3 into 17–19 kDa fragments significantly increased in THDF-treated cells (Figure 3A) and in accordance with this result, PARP protein which is normally involved in DNA repair and a known substrate for caspase-3, was effectively hydrolyzed to the 85 kDa fragment. As shown in Figure 3A, concentrations of THDF as low as 3 μM significantly promote procaspase-7, -6, and -3 hydrolysis. Protein loading was checked by reprobing the membranes with β-actin antibody.

Release of cytochrome *c* from mitochondria to cytosol is a central event in apoptotic signaling. To determine whether THDF-induced apoptosis involves cytochrome *c* release, cytosolic and mitochondrial preparations were analyzed by immunoblotting on HL-60 and U937 cell lines. The results show a significant increase in the amount of cytochrome *c* in the cytosol, which was correlated with a decrease in the mitochondria, in a concentration- and time-dependent manner (Figure 3A).

The intrinsic pathway is controlled by the Bcl-2 protein family. Bcl-2 itself and Bax inhibits and promotes apoptosis, respectively. We also investi-

Table 1. Effects of THDF on the Growth of Human Tumor Cell Lines

IC_{50} (μM)								
HL-60	HL-60/neo	HL-60/Bcl-x_L	U-937	U-937/Bcl-2	Jurkat	Molt-3	SK-MEL-1	A-549
0.30 ± 0.02	0.59 ± 0.02	3.0 ± 1.2	1.4 ± 0.5	4.3 ± 1.7	0.43 ± 0.05	0.27 ± 0.01	13.9 ± 2.5	10.8 ± 2.4

Cells were cultured for 72 h and the IC_{50} values were calculated as described in the Materials and Methods Section. The data shown represent the means ± SE of 3–5 independent experiments with three determinations in each.

gated the expression of these proteins in THDF-treated cells. Although, there were no clear changes in Bcl-2 levels, cleavage of this antiapoptotic factor was observed in both cell lines (Figure 3A, central panel). Bax may play a crucial role in the apoptotic process via a number of different mechanisms. For instance, Bcl-2 or Bcl-x_L counteracts the effect of Bax by forming heterodimers with it. Previous studies have shown that the ratio between proapoptotic and antiapoptotic Bcl-2 families plays a major role in determining susceptibility of cells to apoptotic stimuli [19,20]. When HL-60 and U937 cells were exposed to THDF a clear decrease in Bax levels in the cytosolic fraction was observed, but there were no significant changes in the mitochondrial fraction in the assayed conditions (Figure 3A, central panel).

As processing does not always correlate with activity, enzymatic activity of caspase-3-like protease (caspase-3/7) was also investigated in extracts of HL-60 cells treated during different time durations or with different concentrations of THDF. Cell lysates were assayed for cleavage of the tetrapeptide substrate DEVD-*p*NA as specific substrate for caspase-3/7. As shown (Figure 3B), induction of caspase-3 like activity was significantly detectable after 12 h of treatment and increased with the incubation time. Dose–response experiments show that a low concentration (1 μM) of THDF was sufficient to induce caspase-3/7 activation (Figure 3C). To confirm that THDF-triggered apoptosis requires the activation of caspases, cells were pretreated with the broad-spectrum caspase inhibitor z-VAD-fmk. The results (Figure 3D) show that apoptosis was almost completely suppressed in the presence of the inhibitor, which suggests that THDF induces cytotoxicity by a caspase-dependent mechanism.

Overexpression of the Mitochondrial Proteins Bcl-2 and Bcl-x_L Confers Partial Resistance to THDF-Induced Apoptosis

Since Bcl-2 and Bcl-x_L are known to inhibit apoptosis by regulating mitochondrial membrane potential and cytochrome *c* release needed for the activation of caspase-9, we decided to clarify whether these proteins protect cells against the effects of THDF. To this end we used cell lines overexpressing Bcl-x_L (HL-60/Bcl-x_L) or Bcl-2 (U937/Bcl-2). Our results indicate that the overexpression of both factors partially blocked THDF-induced cell death and apoptosis, as determined by the 3-(4,5-dimethyl-2-thyazolyl-)-2,5-diphenyl-2*H*-tetrazolium bromide (MTT) assay (Table 1) and flow cytometry experiments (Figure 3E).

The dissipation of the electrochemical gradient ($\Delta\Psi_m$) created by the proteins of the respiratory chain located on the inner mitochondrial membrane

Table 2. Effect of Different Durations of Treatment With THDF on Cell-Cycle Phase Distribution of HL-60 and U937 Cells

		% Sub-G_1	% G_1	% S	% G_2–M
HL-60 (h)					
6	Control	5.7 ± 0.6	40.6 ± 2.4	21.6 ± 0.8	33.3 ± 3.6
	THDF	6.3 ± 2.2	28.4 ± 4.5*	23.1 ± 2.2	42.8 ± 4.8*
12	Control	4.3 ± 1.5	46.6 ± 3.3	24.9 ± 2.6	25.1 ± 3.1
	THDF	11.3 ± 3.4*	22.5 ± 2.5*	16.5 ± 5.1	44.3 ± 0.5*
24	Control	4.4 ± 1.8	46.8 ± 3.1	23.9 ± 2.3	25.4 ± 2.9
	THDF	21.5 ± 3.8*	30.6 ± 1.7*	17.8 ± 3.9*	26.5 ± 1.0*
U937 (h)					
6	Control	4.9 ± 1.9	48.8 ± 3.6	20.4 ± 1.5	24.1 ± 4.6
	THDF	5.0 ± 1.3	36.5 ± 2.1*	22.6 ± 0.8	33.4 ± 5.3*
12	Control	4.8 ± 1.1	51.8 ± 5.2	20.3 ± 2.5	22.4 ± 3.0
	THDF	23.6 ± 4.8*	20.5 ± 5.5*	10.1 ± 3.6	38.6 ± 8.7*
24	Control	5.4 ± 1.5	51.3 ± 3.6	19.7 ± 2.4	22.6 ± 2.1
	THDF	21.4 ± 0.6*	20.9 ± 0.6*	14.6 ± 4.6	35.8 ± 3.2*

Cells were cultured with 3 μM THDF for the indicated period of times and the cell-cycle phase distribution was determined by flow cytometry. The values are means ± SE of two independent experiments with two determinations in each. Asterisks indicate a significant difference ($P < 0.05$) compared with the corresponding controls.

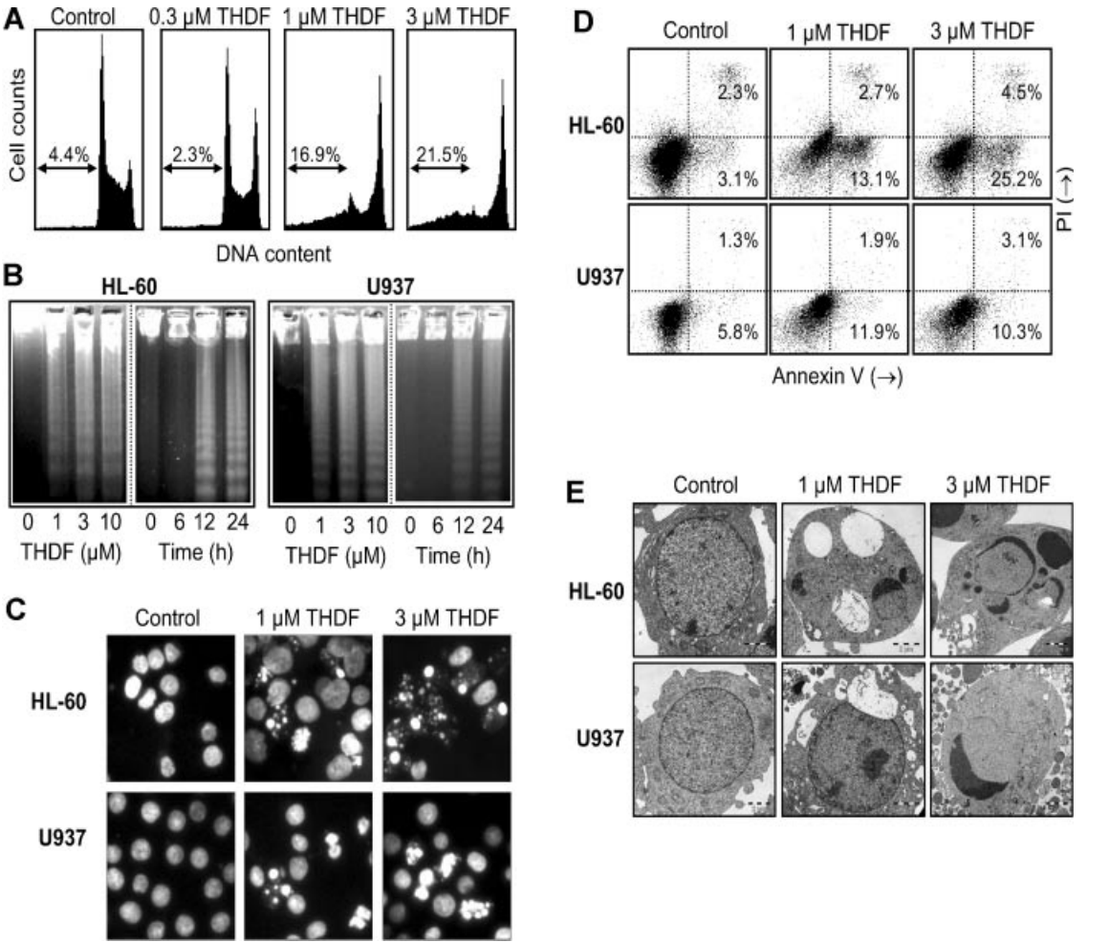

Figure 2. Effects of THDF on apoptosis on human myeloid leukemia HL-60 and U937 cells. (A) HL-60 cells were incubated in the presence of the indicated concentrations of THDF and subjected to flow cytometric analysis. Hypodiploid cells (apoptotic cells) are shown in region marked with an arrow. (B) Dose–response and kinetics of DNA fragmentation in response to THDF. HL-60 and U937 cells were incubated in the presence of the indicated concentrations of THDF for 24 h or were treated with 3 μM THDF and harvested at the indicated times and genomic DNA was extracted, separated on an agarose gel, and visualized under UV light by ethidium bromide staining. (C) Photomicrographs of representative fields of HL-60 and U937 cells stained with Hoechst 33258 to evaluate nuclear chromatin condensation (i.e., apoptosis) after treatment with THDF. (D) FACS analysis of Annexin V-FITC and propidium iodide (PI)-stained HL-60 and U937 cells after 24 h of treatment with the indicated concentrations of THDF. Cells appearing in the lower right quadrant show positive Annexin V-FITC staining, which indicates phosphatidylserine translocation to the cell surface, and negative PI staining, which demonstrates intact cell membranes, both features of early apoptosis. Cells in the top right quadrant are double positive for Annexin V-FITC and PI and are undergoing necrosis. Data are representative of three separate experiments. (E) Transmission electron micrographs of HL-60 and U937 cells after 24 h incubation with the indicated concentrations of THDF.

is also a key event in mitochondria-controlled apoptotic pathways. To examine whether a disruption of the $\Delta\Psi_m$ is required for the release of cytochrome *c*, cells were treated with THDF for different times (6, 12, and 24 h), stained with JC-1 and analyzed by flow cytometry. The results (Figure 3F) indicate that $\Delta\Psi_m$ dropped at 12 h of treatment, which suggests that the disruption of the mitochondrial membrane potential is associated in THDF-induced apoptosis.

THDF Activates Mitogen-Activated Protein Kinases (MAPKs)

In view of evidence that the MAPKs play a critical role in cell fate, the effects of THDF on the activation of these signaling pathways were examined. As shown (Figure 4A) this compound leads to phosphorylation of JNK/SAPK, p38 MAPKs ($p38^{MAPK}$) on HL-60 and U937, while phosphorylation of ERK1/2 was only observed in HL-60. Phosphorylation of $p38^{MAPK}$ was detected 15 min after THDF addition and remained elevated for at least 6 h (Figure 4A). However, the activation of JNK/SAPK was not observed until 1 and 2 h in U937 and HL-60 cells, respectively, under the same experimental conditions (Figure 4A). The level of phosphorylated ERK1/2 increased after 15 min and returned to the control level at 1 h (initial peak). Two hours after THDF addition, the levels of phosphorylated ERK1/2 increased again for at least 6 h (Figure 4A). These

results indicate that the ERK1/2 pathway is activated rapidly in response to THDF in HL-60 cells, and that this activation occurs in a biphasic manner. Therefore, THDF leads to activation of JNK/SAPK, p38^{MAPK}, and ERK1/2 following different kinetics. It is important to note that the changes in the phosphorylation state of MAPKs were only investigated until 6 h after exposure to THDF. Taking into account that THDF

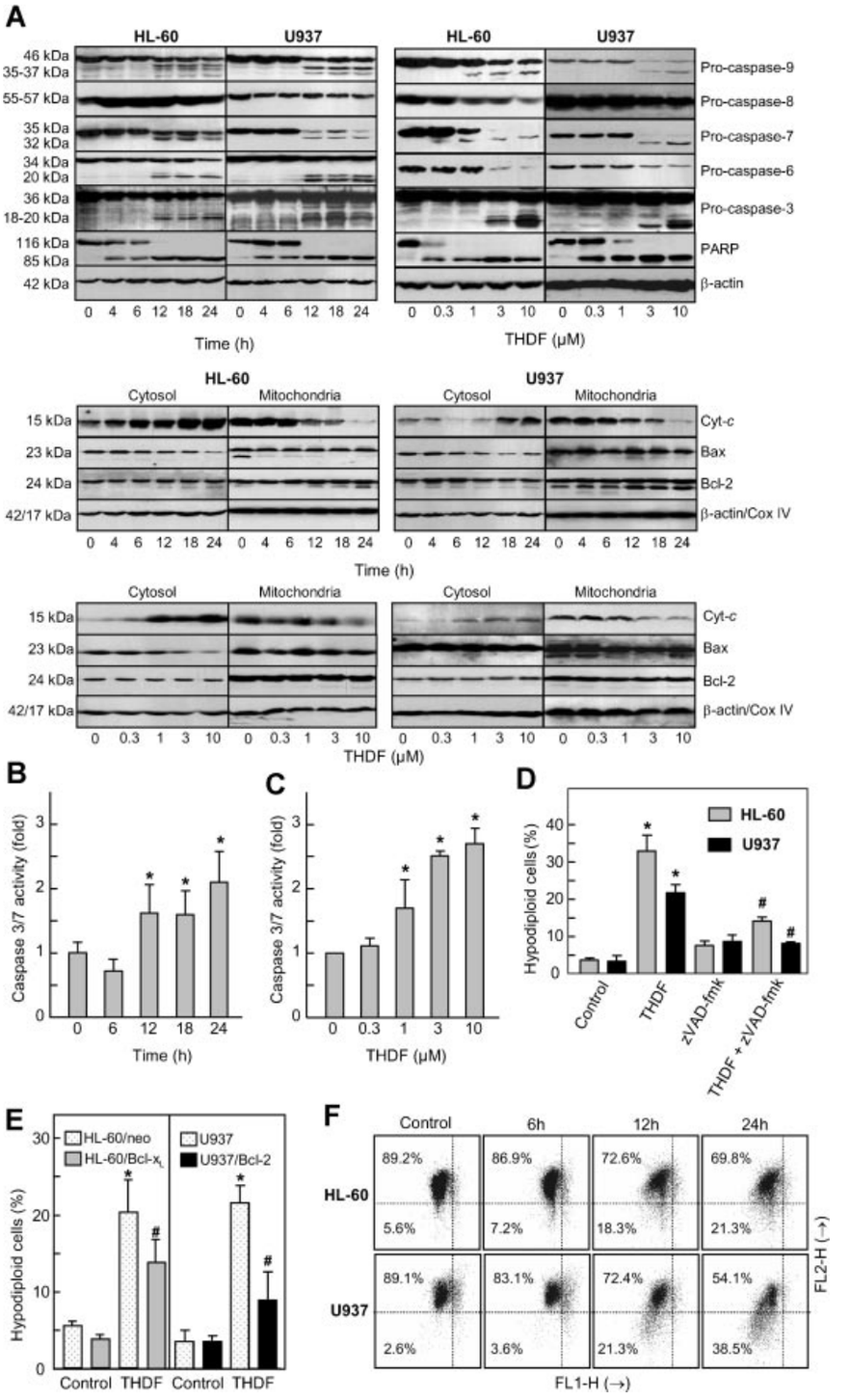

Figure 3.

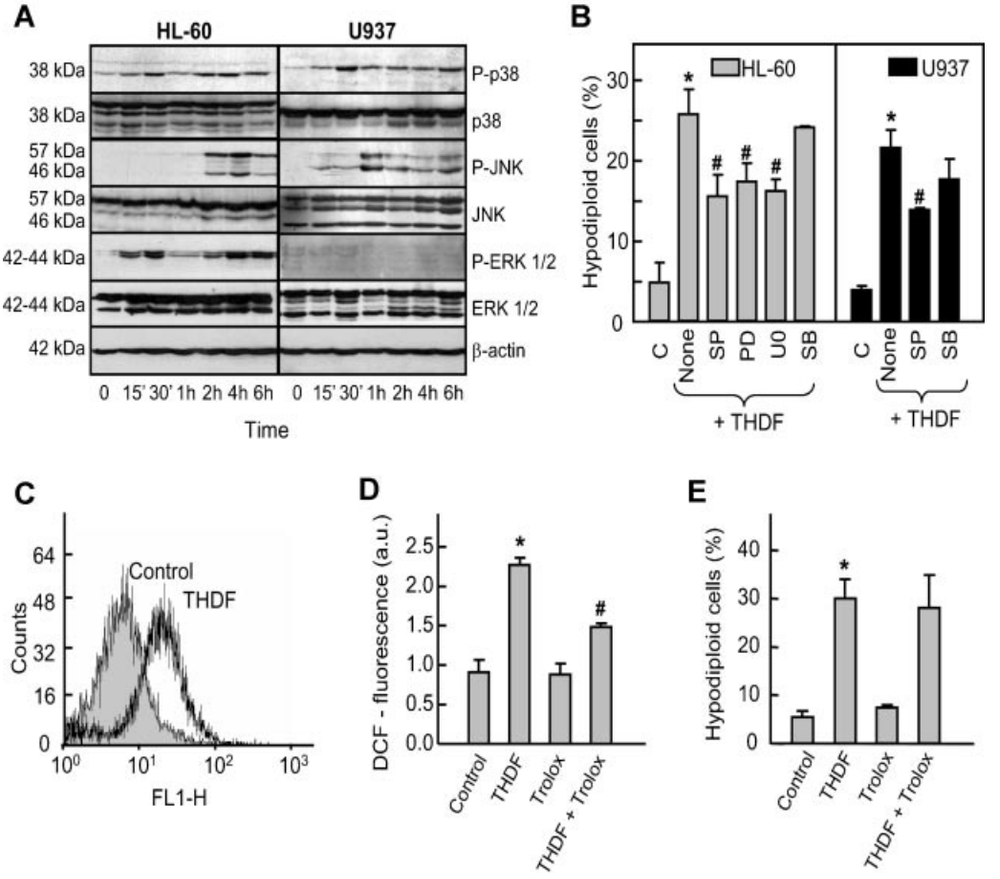

Figure 4. THDF induces phosphorylation of MAPKs and ROS generation. (A) Representative Western blots show the time-dependent phosphorylation of $p38^{MAPK}$, JNK/SAPK, and ERK1/2 by THDF. HL-60 and U937 cells were incubated with THDF for the indicated time points. Protein extracts were prepared and analyzed on Western blots probed with specific antibodies to ascertain the phosphorylation of MAPKs. Membranes were stripped and reprobed with total $p38^{MAPK}$, JNK/SAPK, ERK1/2, and β-actin antibodies as loading controls. (B) Cells were preincubated with SP600125 (SP, 10 μM), PD98059 (PD, 10 μM), U0126 (U0, 10 μM), and SB203580 (SB, 2 μM) for 1 h and then treated with THDF. Apoptosis was quantified by flow cytometry and bars represent the means ± SE of three independent experiments each performed in triplicate. (C) THDF increases ROS generation. HL-60 cells were treated with 10 μM THDF for 1 h and the fluorescence of oxidized H_2-DCF was determined by flow cytometry. Similar results were obtained from three independent experiments. (D) Cells were pretreated with Trolox (2 mM) for 1 h and then incubated with THDF for 24 h and intracellular ROS levels were determined as above. (E) Cells were pretreated with Trolox and then exposed to THDF (3 μM) for 24 h. Hypodiploid cells were determined by flow cytometry. Values represent means ± SE of three independent experiments each performed in triplicate. $^{*}P < 0.05$, significantly different from untreated control. $^{\#}P < 0.05$, significantly different from THDF treatment alone.

Figure 3. Evaluation of apoptotic pathways triggered by THDF on human leukemia cells. (A) HL-60 and U937 cells were incubated in the presence of 3 μM THDF for the indicated times or incubated with the indicated concentrations of THDF for 24 h. Cell lysates were assayed by immunoblotting. β-Actin and Cox IV (cytochrome c oxidase) were used as loading controls in cytosol and mitochondria, respectively. The cytosolic and mitochondria-enriched fractions were prepared and Western blot analyses were performed as described in the Materials and Methods Section. (B) HL-60 cells were treated with 3 μM THDF and harvested at the indicated times. Cell lysates were assayed for caspase-3 and -7 activity using the DEVD-*p*NA colorimetric substrates. Results are expressed as factorial increases in caspase activity compared with the control. Values represent means ± SE of two independent experiments each performed in triplicate. (C) Dose–response experiments of caspase-3/7 activation in response to THDF. HL-60 cells were treated with the indicated concentrations of THDF and cell lysates were assayed for caspase-3 and -7 activities as above. (D) HL-60 and U937 cells were pretreated with z-VAD-fmk (100 μM) before the addition of THDF (3 μM) for 24 h, and apoptotic cells were analyzed by flow cytometry after staining with propidium iodide. Values represent the means ± SE of three independent experiments each performed in triplicate. $^{*}P < 0.05$, significantly different from untreated control. $^{\#}P < 0.05$, significantly different from THDF treatment alone. (E) Effect of THDF on cells overexpressing Bcl-x_L and Bcl-2. Comparison of THDF treatment in HL-60/neo and HL-60/Bcl-x_L cells, and also in U937 and U937/Bcl-2 cells. The percentage of hypodiploid cells was determined by flow cytometry at 24 h in the absence or presence of 3 μM THDF. Values represent means ± SE of three different experiments. $^{*}P < 0.05$, significantly different from untreated control. (F) THDF reduces the mitochondrial membrane potential ($\Delta\Psi_m$). HL-60 and U937 cells were treated with 1 μM THDF and harvested at indicated times and $\Delta\Psi_m$ analyzed with JC-1. The intensity of JC-1 fluorescence was analyzed by flow cytometry as described in the Materials and Methods Section. Similar results were obtained in two separate experiments each performed in triplicate.

induces significant cell death after 12 h, we analyzed the changes in the phosphorylation state of MAPKs prior to this in order to evaluate the early changes caused by THDF rather nonspecific changes associated with apoptosis. To determine whether the phosphorylation of MAPKs plays a key role in THDF-induced apoptosis, we examined the effects of specific inhibitors. Therefore, pretreatment of cells with SB203580 (2 μM) did not alter significantly the rate of THDF-mediated apoptosis (Figure 4B), which suggest that $p38^{MAPK}$ activation is not involved. However, preincubation with the specific JNK/SAPK inhibitor SP600125 (10 μM) partially blocked THDF-mediated apoptosis in both cell lines.

We also investigated the putative impact of ERK1/2 on the signal transduction pathway leading to THDF-mediated cell death. For this purpose, we used specific mitogen-activated extracellular kinase 1/2 (MEK1/2) inhibitors in order to block the activation of ERK1/2. The results indicate that PD98059 and U0126 significantly attenuated THDF-induced cell death (Figure 4B).

THDF Increases Intracellular ROS Levels

Generation of intracellular ROS is considered one of the key mediators of apoptotic signaling for the most antitumoral agents. Therefore, the redox status of HL-60 cells was monitored by the oxidation-sensitive fluorescent dye H_2-DCF-DA. The results show a fast generation of ROS after 15 min (results not shown) of treatment with THDF, although the highest levels (~2.2-fold increase compared with control) were not reached until 1 h (Figure 4C). For comparison, exposure to H_2O_2 (100 μM) was associated with a quick increase in ROS levels (5 min) that decreased after 1 h of treatment (results not shown). We next investigated whether oxidative stress is essential for THDF-mediated apoptosis. To explore this possibility cells were pretreated with different antioxidants, including trolox (2 mM), the glutathione precursor *N*-acetyl-L-cysteine (NAC, 10 mM), α-tocopherol (vitamin E, 25 μM), the inhibitor of xanthine oxidase allopurinol (100 μM), ascorbic acid (vitamin C, 100 μM), and the ROS degrading enzymes catalase (400 U/mL) and superoxide dismutase (SOD, 400 U/mL). Trolox was the only antioxidant in decreasing the generation of ROS, but it was unable to block cell death (Figure 4D and E). These findings suggest that THDF-induced apoptosis is independent of ROS generation.

DISCUSSION

While there are effective treatments for acute lymphocytic leukemia and for chronic myelogenous leukemia, more effective treatments for other forms of acute leukemia are needed. Polyphenolic compounds are of great current interest due to their possible anticancer activities [1]. In previous studies with naturally occurring and semisynthetic phenylbenzo-γ-pyrones, we showed that methylation of hydroxyl group at position C3 of quercetin yields a compound with a higher antiproliferative activity in several cancer cell lines [13]. We have also demonstrated that betuletol 3-methyl ether, a natural flavonoid, is a potent inhibitor of proliferation which displays high cytotoxic activity on human myeloid leukemia HL-60 cells [13].

In this study we have specifically selected an analog of quercetin 3-methyl ether, THDF, which contains an additional methoxyl group on position 4′ of the phenylbenzo-γ-pyrone core and evaluated its potential cytotoxic properties using nine tumor cell lines. Interestingly, we found that THDF displays cytotoxic properties in a cell-type specific manner. Human leukemia cells (HL-60, U937, Molt-3, and Jurkat) were highly sensitive to THDF cytotoxicity while SK-MEL-1 and A549 cells were more resistant than hematopoietic cells. Moreover, dose–response studies revealed that PBMC were more resistant to THDF than PBMC treated with PHA. Cell-cycle analysis showed that inhibition of cell viability by THDF was caused by a significant cell-cycle arrest at the G_2–M phase, accompanied by an increase in sub-G_1 fraction and phosphatidylserine externalization, indicating apoptotic cell death. Similar results were recently reported by the semisynthetic quercetin 3-methyl ether tetracetate in human leukemia cells [15], although the potency of THDF was the highest, both in arresting the cells at the G_2–M phase and as an apoptotic inducer. The arrest of cells in the G_2–M phase of the cell cycle induced by THDF might be explained by the inhibition of microtubule formation or by changes in the expression and/or activity of G_2–M cell-cycle regulators. Further studies are needed to determine the effect of this compound on these regulators such as the cyclin-dependent kinase-1, cyclin-dependent kinase inhibitor $p21^{Cip1}$, B-type cyclin isoforms, and cdc25C.

Our results also indicate that THDF's antiproliferative effect is dependent on caspase, since cell death was inhibited by the general caspase inhibitor z-VAD-fmk. The intrinsic apoptotic pathway (mitochondrial pathway) involves the release of cytochrome *c* and the assembly of apoptosome. THDF initiated redistribution of cytochrome *c* into the cytosol which was correlated with the dissipation of $\Delta\Psi_m$ and caspase-3 activation. We also observed a concentration- and time-dependent activation of caspase-9 and -3, in accordance with the cytochrome *c* release experiments, emphasizing that the intrinsic pathway plays an important role in the cell death. Moreover, THDF induced PARP cleavage, a hallmark of apoptosis that indicates activation of caspase. Although PARP is also degraded in other forms of cell death like necrosis [21], this did not seem to be the case with THDF in accordance with the fluorescence microscopy and the flow cytometric analyses of

Annexin V-FITC and propidium-iodide-stained cells experiments. The results clearly demonstrate that THDF also stimulates the proteolytic processing of other executioner caspases, namely caspase-7 and -6 to form activated enzymes.

There was also a clear concentration- and time-dependent decrease of the Bax levels in the cytosol in both cell lines. However, the levels of Bcl-2 in mitochondria and in cytosol remain unchanged. Therefore, it appears that the mechanism of cytotoxicity displayed by THDF is clearly different to that caused by previously described phenylbenzo-γ-pyrones, such as betuletol 3-methyl ether which induces apoptosis in HL-60 cells by a caspase-8-dependent mechanism [13]. In contrast, quercetin 3-methyl ether tetracetate, a flavonoid obtained by acetylation of the natural product quercetin 3-methyl ether, triggers apoptosis which is prevented by the general caspase inhibitor z-VAD-fmk, but not by the specific caspase-8 inhibitor [15].

Previous studies have shown that increased expression of Bcl-2 and/or Bcl-x_L is associated with chemoresistance particularly in the case of hematologic malignancies [22] and there is also poor prognostic outcome with increased Bcl-x_L expression [23]. To further investigate the role of mitochondria in THDF-induced cytotoxicity, HL-60 and U937 cells overexpressing antiapoptotic factors were included in this study. Our results indicate that HL-60/Bcl-x_L and U937/Bcl-2 were partially resistant compared with the parental cell lines, which suggest that mitochondria play an important role in THDF-induced cell death. However, the partial protection by these proteins could be explained by various mechanisms, including inactivation of Bcl-2 or the activation of the extrinsic apoptotic pathway. The fact that THDF induces cell death also in leukemic cells overexpressing Bcl-2 and Bcl-x_L could have important clinical implications for the use of this compound as potential therapeutic agent.

Recent studies suggest that MAPKs such as JNK/SAPK and $p38^{MAPK}$ play a key role in triggering apoptosis in response to various cellular stressors including oxidative stress [24]. The $p38^{MAPK}$ is activated by a variety of cellular stresses including ultraviolet light, hyperosmolarity, heat shock, and proinflammatory cytokines, and acts at early step prior to dysfuction of mitochondria and caspase activation. Moreover, $p38^{MAPK}$ is a potential upstream regulator of Bax [25] and a mediator of the G_2–M checkpoint response [26]. In this regard, activation of $p38^{MAPK}$ in mammalian cells in response to the disruption of the microtubule cytoskeleton initiates G_2–M checkpoint [27] and also previous studies have shown that flavonoids containing a 3-methoxyl group may inhibit tubulin polymerization [28]. Although our studies indicate that the activation of $p38^{MAPK}$ is not involved in THDF-induced cell death, this could be involved in the initiation of the G_2–M checkpoint through a perturbation of the microtubules.

A proapoptotic role of JNK has been described in apoptosis induced by different chemotherapeutic agents, such as vinblastine, doxorubicin, and etoposide [29,30]. Furthermore, 2-methoxyestradiol-induced apoptosis was inhibited by SP600125 in multiple myeloma cells [31]. In this study we show that THDF-induced cell death was also associated with the phosphorylation of the members of MAPKs following different kinetics and this effect was cell specific, since ERK1/2 activation was observed in HL-60 but not in U937 cells. Moreover, THDF induced a biphasic phosphorylation of ERK1/2. Although the mechanisms by which THDF caused this response is unknown, one possible explanation could be the involvement of dual specificity threonine/tyrosine MAPK phosphatases (MKPs) because some of these MKPs are encoded by genes that are transcriptionally activated by ERK1/2 and this can provide a feedback loop to downregulate ERK1/2 activity [32]. In addition, the enzymatic activity of MKPs is sensitive to reversible oxidation and inactivation due to the presence of the catalytic cysteine residue in the catalytic cleft [33]. The reversible oxidation of this cysteine residue that inactivates the phosphatase may be mediated by the generation of ROS such as H_2O_2 [34]. THDF induces ROS and might inhibit the MKPs and therefore explain the second peak of ERK activation triggered by THDF. Another possible explanation could be that the early activation of ERK1/2 may enhance the expression of potential targets, which amplify the THDF response and induce a secondary phosphorylation of ERK1/2, as previously reported for transforming growth factor-β-1 [35].

Although the JNK pathway has been shown to be closely linked to apoptosis [12], its exact role seems to depend on the cell type and stimulus. Interestingly, in HL-60 the percentage of hypodiploid cells in response to THDF was attenuated by inhibition of JNK/SAPK and by inhibition of ERK1/2, which suggests that both MAPKs are required for cell death.

Our results also indicate that the MEK1/2 inhibitors PD98059 and U0126 attenuated the apoptotic effects of THDF, which suggest that ERK1/2 is involved in cell death signals. These findings are in agreement with previous work that has shown that inhibition of MEK-ERK activation with U0126 or PD98059 abolishes quercetin-induced apoptosis in A549 cells [36]. In addition, we have recently shown that inhibition of ERK1/2 attenuates cell death induced by the acetyl derivative of the flavonoid trifolin [17] and by the naturally occurring flavonoid betuletol 3-methyl ether [37].

ROS have been implicated as second messengers in multiple signaling pathways [38]. Although the antiproliferative effect of THDF is associated with an increase in the intracellular level of ROS, this did not

seem to play a pivotal role in the apoptotic process. The generation of ROS is not a general feature of polyphenolic compounds containing a phenyl-benzo-γ-pyrone core. In this regard, we have previously demonstrated that quercetin 3-methyl ether tetracetate induces apoptosis in human leukemia cells without ROS formation [15], while that trifolin acetate induces ROS, but they are not necessary to trigger cell death [17].

In conclusion, we describe a potent analog of quercetin that induces cytotoxicity via G_2–M phase cell-cycle arrest and apoptosis through a caspase-dependent mechanism involving mitochondria and MAPK. Our study reveals details about the signaling pathways triggered by THDF in human leukemia cells. Based on the present findings, we suggest that this flavonoid may be useful in the development of new therapeutic agents against cancer.

ACKNOWLEDGMENTS

We thank J. Estévez (Hospital Universitario Insular de Gran Canaria) for his collaboration in the Western blot assays and to the Electronic Microscopy Service of the University of Las Palmas de Gran Canaria. F.T. was supported by a research studentship from the Canary Islands Government. This work was supported by Grants from the Ministry of Education and Science of Spain and from the European Regional Development Fund (SAF2007-62536) and from the Canary Islands Government (PI 2007/045 to J.Q.).

REFERENCES

1. Middleton E, Kandaswami C, Theoharides TC. The effects of plant flavonoids on mammalian cells: Implications for inflammation, heart disease, and cancer. Pharmacol Rev 2000;52:673–751.
2. Teofili L, Pierelli L, Iovino MS, et al. The combination of quercetin and cytosine arabinoside synergistically inhibits leukemic cell growth. Leuk Res 1992;16:497–503.
3. Wei YQ, Zhao X, Kariya Y, Fukata H, Teshigawara K, Uchida A. Induction of apoptosis by quercetin: Involvement of heat shock protein. Cancer Res 1994;54:4952–4957.
4. Thornberry NA, Lazebnik Y. Caspases: Enemies within. Science 1998;281:1312–1316.
5. Boatright KM, Salvesen GS. Mechanisms of caspase activation. Curr Opin Cell Biol 2003;15:725–731.
6. Nagata S. Apoptosis by death factor. Cell 1997;88:355–365.
7. Cohen GM. Caspases: The executioners of apoptosis. Biochem J 1997;326:1–16.
8. Breckenridge DG, Germain M, Mathai JP, Nguyen M, Shore GC. Regulation of apoptosis by endoplasmic reticulum pathways. Oncogene 2003;22:8608–8618.
9. Chipuk JE, Green DR. Do inducers of apoptosis trigger caspase-independent cell death? Nat Rev Mol Cell Biol 2005; 6:268–275.
10. Raman M, Chen W, Cobb MH. Differential regulation and properties of MAPKs. Oncogene 2007;26:3100–3112.
11. Verheij M, Bose R, Lin XH, et al. Requirement for ceramide-initiated SAPK/JNK signalling in stress-induced apoptosis. Nature 1996;380:75–79.
12. Davis RJ. Signal transduction by the JNK group of MAP kinases. Cell 2000;103:239–252.
13. Rubio S, Quintana J, López M, Eiroa JL, Triana J, Estévez F. Phenylbenzopyrones structure-activity studies identify betuletol derivatives as potential antitumoral agents. Eur J Pharmacol 2006;548:9–20.
14. Torres F, Quintana J, Cabrera J, et al. Induction of G_2–M phase arrest and apoptosis by α-methylene-γ-butyrolactones in human leukaemia cells. Cancer Lett 2008;269:139–147.
15. Rubio S, Quintana J, Eiroa JL, Triana J, Estévez F. Acetyl derivative of quercetin 3-methyl ether-induced cell death in human leukemia cells is amplified by the inhibition of ERK. Carcinogenesis 2007;28:2105–2113.
16. Kaczmarek L, Calabretta B, Baserga R. Expression of cell-cycle-dependent genes in phytohemagglutinin-stimulated human lymphocytes. Proc Natl Acad Sci USA 1985;82:5375–5379.
17. Torres F, Quintana J, Díaz JG, Carmona AJ, Estévez F. Trifolin acetate-induced cell death in human leukaemia cells is dependent on caspase-6 and activates the MAPK pathway. Apoptosis 2008;13:716–728.
18. De Lean A, Munson PJ, Rodbard D. Simultaneous analysis of families of sigmoidal curves: Application to bioassay, radioligand assay, and physiological dose-response curves. Am J Physiol 1978;235:E97–E102.
19. Zhang L, Yu J, Park BH, Kinzler KW, Vogelstein B. Role of BAX in the apoptotic response to anticancer agents. Science 2000;290:989–992.
20. Perlman H, Zhang X, Chen MW, Walsh K, Buttyan R. An elevated bax/bcl-2 ratio corresponds with the onset of prostate epithelial cell apoptosis. Cell Death Differ 1999;6: 48–54.
21. Soldani C, Scovassi AI. Poly(ADP-ribose) polymerase-1 cleavage during apoptosis: An update. Apoptosis 2002;7: 321–328.
22. Amundson SA, Myers TG, Scudiero D, Kitada S, Reed JC, Fornace AJ, Jr. An informatics approach identifying markers of chemosensitivity in human cancer cell lines. Cancer Res 2000;60:6101–6110.
23. Addeo R, Caraglia M, Baldi A, et al. Prognostic role of bcl-xL and p53 in childhood acute lymphoblastic leukemia (ALL). Cancer Biol Ther 2005;4:32–38.
24. Tobiume K, Matsuzawa A, Takahashi T, et al. ASK1 is required for sustained activations of JNK/p38 MAP kinases and apoptosis. EMBO Rep 2001;2:222–228.
25. Ghatan S, Larner S, Kinoshita Y, et al. p38 MAP kinase mediates bax translocation in nitric oxide-induced apoptosis in neurons. J Cell Biol 2000;150:335–347.
26. Bulavin DV, Higashimoto Y, Popoff IJ, et al. Initiation of a G2/M checkpoint after ultraviolet radiation requires p38 kinase. Nature 2001;411:102–107.
27. Matsusaka T, Pines J. Chfr acts with the p38 stress kinases to block entry to mitosis in mammalian cells. J Cell Biol 2004; 166:507–516.
28. Beutler JA, Hamel E, Vlietinck AJ, et al. Structure-activity requirements for flavone cytotoxicity and binding to tubulin. J Med Chem 1998;41:2333–2338.
29. Brantley-Finley C, Lyle CS, Du L, et al. The JNK, ERK and p53 pathways play distinct roles in apoptosis mediated by the antitumor agents vinblastine, doxorubicin, and etoposide. Biochem Pharmacol 2003;66:459–469.
30. Mingo-Sion AM, Marietta PM, Koller E, Wolf DM, Van Den Berg CL. Inhibition of JNK reduces G2/M transit independent of p53, leading to endoreduplication, decreased proliferation, and apoptosis in breast cancer cells. Oncogene 2004; 23:596–604.
31. Chauhan D, Li G. JNK-dependent release of mitochondrial protein, Smac, during apoptosis in multiple myeloma (MM) cells. J Biol Chem 2003;278:17593–17596.
32. Owens DM, Keyse SM. Differential regulation of MAP kinase signalling by dual-specificity protein phosphatases. Oncogene 2007;26:3203–3213.
33. Kamata H, Honda S, Maeda S, Chang L, Hirata H, Karin M. Reactive oxygen species promote TNFα-induced death and

sustained JNK activation by inhibiting MAP kinase phosphatases. Cell 2005;120:649–661.
34. Tonks NK. Redox redux: Revisiting PTPs and the control of cell signaling. Cell 2005;121:667–670.
35. Lien S-C, Usami S, Chien S, Chiu J-J. Phosphatidylinositol 3-kinase/Akt pathway is involved in transforming growth factor-β1-induced phenotypic modulation of 10T1/2 cells to smooth muscle cells. Cell Signal 2006;18:1270–1278.
36. Nguyen TTT, Tran E, Nguyen TH, Do PT, Huynh TH, Huynh H. The role of activated MEK-ERK pathway in quercetin-induced growth inhibition and apoptosis in A549 lung cancer cells. Carcinogenesis 2004;25:647–659.
37. Rubio S, Quintana J, Eiroa JL, Triana J, Estévez F. Betuletol 3-methyl ether induces G_2–M phase arrest and activates the sphingomyelin and MAPK pathways in human leukemia cells. Mol Carcinog 2010;49:32–43.
38. Apel K, Hirt H. Reactive oxygen species: Metabolism, oxidative stress, and signal transduction. Annu Rev Plant Biol 2004;55:373–399.